Lubricant-free deep drawing using CO_2 and N_2 as volatile media injected through laser-drilled microholes

Ehsan Zahedi[1,], Christoph Woerz[2], Gerd Reichardt[2], Georg Umlauf[3], Mathias Liewald[2], Jakob Barz[3], Rudolf Weber[1], Thomas Graf[1]*

[1]Institut für Strahlwerkzeuge, Universität Stuttgart, Pfaffenwaldring 43, 70569 Stuttgart, Germany
[2]Institut für Umformtechnik, Holzgartenstraße 17, 70174 Stuttgart, Germany
[3]Fraunhofer Institute for Interfacial Engineering and Biotechnology, Fraunhofer IGB, Nobelstraße 12, 70569 Stuttgart, Germany

Abstract. Most metal forming processes use lubricants based on mineral oils as an intermediate medium to reduce friction and wear. To avoid the well-known drawbacks of oil lubrication, a novel and environment friendly lubrication system for deep-drawing processes was demonstrated at the University of Stuttgart. Liquid carbon dioxide and gaseous nitrogen are being used as volatile lubrication during the deep-drawing process, locally injected at high pressure through laser-drilled microholes. This new tribological system provides a significantly enlarged working range and at least 15% larger drawing depths compared to conventional oil lubrication.

Keywords: Deep drawing, Laser micro machining, Drilling.

1. INTRODUCTION

In metal deep-drawing, usually mineral oil- or wax-based lubricants are used. These lubricants may contain toxic additives, and the formed components have to be cleaned in subsequent process steps in a cost and time-consuming manner [1]. To avoid these issues, a novel tribological system for sheet metal deep drawing that eliminates the use of conventional lubricants was developed at the University of Stuttgart. A sketch of the process is shown in Figure 1.

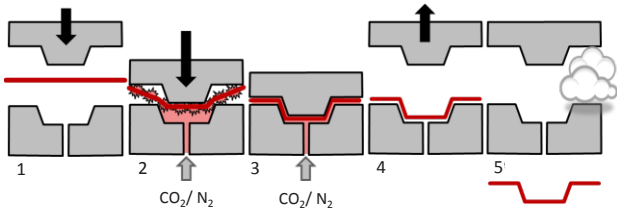

Figure 1. Sketch of the forming process using volatile fluids as lubricant.

During the forming of the material, liquid CO_2 or N_2 is supplied at high pressure through diffusor-shaped, laser-drilled microholes. The liquid gas that evaporates close before or in the contact zone between sheet metal and tool surface, serves as lubricant, and subsequently evaporates without residue.
This paper summarizes the results achieved in the three basic contributions from the institutes involved. This includes (1) the flow behaviour of N_2 and CO_2 for different hole geometries, (2) the basic issues for laser drilling of shaped deep microholes, and (3) fundamental deep drawing tests with rectangular cups to demonstrate the capability of volatile lubricants. A CAD-drawing of a cross section through the segmented die of the deep drawing tool is shown in Figure 2.

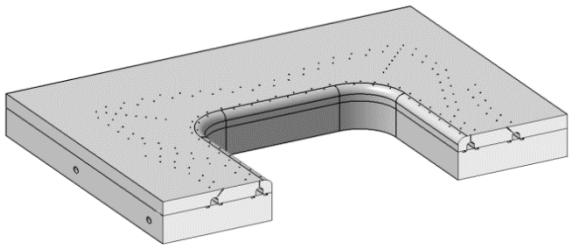

Figure 2. Cross section through the segmented die of the deep drawing tool.

2. PROPERTIES OF CO_2 AND N_2

Since the beginning of the 90s, the use of carbon dioxide as a working medium in refrigeration, air conditioning and heat pump processes has become the focus of technical interest. In the chemical industry CO_2, e.g. as industrial gas, long used as raw material - also as protective gas for packaged food, as fertilizer or for the production of medicines it is used. Finally, in the late 1990s, the discussion on atmospheric greenhouse gas emissions in general and the capture, transport and storage of Carbon Capture and Storage (CCS) in particular became more important. This puts carbon dioxide at the center of technical and political interest.

* Corresponding author: ehsan.zahedi@ifsw.uni-stuttgart.de

First of all, however, another aspect will be briefly discussed: the danger potential associated with the large-scale handling of carbon dioxide. It is well known that carbon dioxide can be toxic and heavier than air. In the past, this has repeatedly resulted in fatal accidents in cellars or feed silos. In fact, the standard density (density at $T_n = 273.15$ K and $p_n = 0.10$ MPa) of carbon dioxide is $\rho_n = 1.97$ kg /m^3. CO_2 is 1.529 times heavier than dry air. However, a dangerous accumulation of escaping carbon dioxide is usually limited to poorly ventilated rooms or cellars. Outdoors, mixing with the moving ambient air takes place quickly. CO_2 is not toxic only by the displacement of atmospheric oxygen, as a metabolite of the body, it also has an immediate effect on vital functions. It should be noted that although the maximum workplace concentration for carbon dioxide is already reached at 0.5% (based on the partial pressure), only concentrations above 20% are lethal in the short-term. While gaseous CO_2 dissolves only a few substances, the solution behavior improves in the liquid and especially in the supercritical state.

Figure 3, shows the p-T diagram of CO_2 and N_2. On the sublimation curve, solid and gas exist simultaneously. Solid and liquid phases exist simultaneously on the melting curve. The sublimation and melting curves coincide with the vapor pressure curve. At the triple point, all three states of matter are gaseous, liquid and firmly in equilibrium [2, 3]. At the upper end of the vapor pressure curve is the critical point. This point is characterized by the critical temperature T_k and the critical pressure p_k. If the temperature and the pressure are increased beyond the critical point, the pure substance is in the supercritical state.

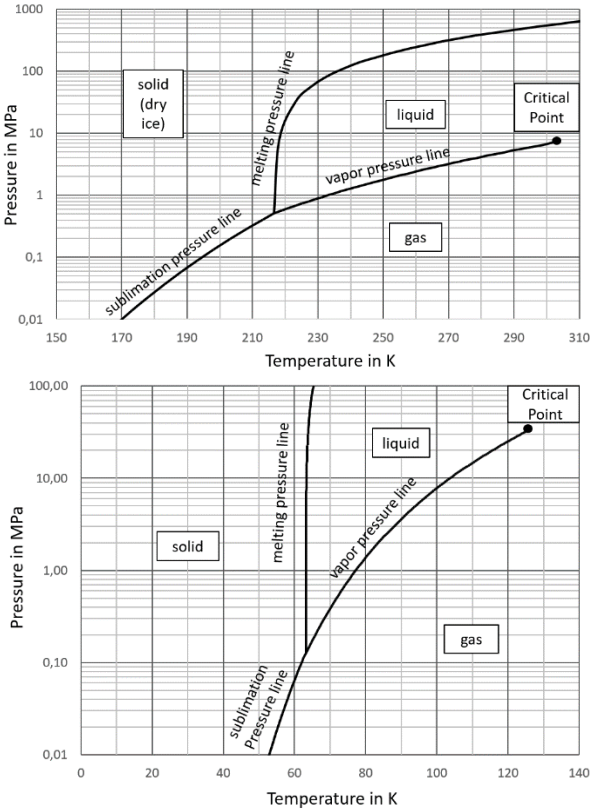

Figure 3. p-T-diagram for CO_2 (upper) and N_2 (bottom).

In contrast, for nitrogen, the critical point for the temperature is 127.15 K and a pressure of 3.39 MPa. This requires that only a strong decrease in temperature at atmospheric pressure can liquefy N_2. A large increase in pressure above 3.39 MPa causes a transition to the supercritical region. In this area, the gas and liquid phases can no longer be separated. In addition, both properties of the states of aggregation are present in parallel. The supercritical state is as dense as a liquid but has the same viscosity as a gas.

Due to the numerous phase transitions in the working window from 1 bar to 60 bar, CO_2 is examined more closely. Nitrogen is in the gaseous state at any point in the processing chain.

Table 1. Comparison of physical properties of CO_2 and N_2.

Property	Value for CO_2	Value for N_2
Crit. Temperature (K)	304.13	126.19
Crit. Pressure (MPa)	7.37	3.39
Crit. Density (kg/m^3)	467.6	313.3
Triple point temperature (K)	216.59	63.15
Triple point pressure (MPa)	0.52	0.01

For these experiments, a CO_2 pressure bottle filled with 6 MPa and a riser is used. This pressure bottle is filled with 60 bar and has a riser.

This pressure bottle is filled with 60 bar and has a riser. Due to the phase differences, the lighter gas phase is above the heavy liquid phase. The bottle is equipped with a riser to insure the state of CO_2 stays liquid in the whole period of time that the bottle has been consumed. When removing the liquid phase flows through the riser upwards, the leads and the microholes directly into the forming tool. The microholes are considered to be open ends and there is atmospheric pressure. It comes to an expansion of the liquid phase. It forms the so-called dry ice in solid form, this can be seen very well by the whitish color as shown in Figure 4. Then sublimates the solid CO_2 in the gas phase.

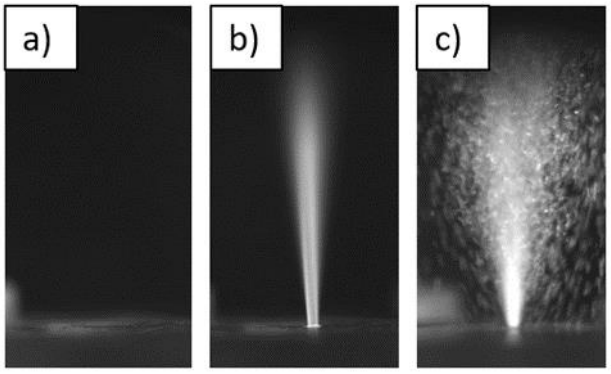

Figure 4. Comparison between the aggregate states gaseous (a), solid (b) and liquid (c) during the flow of CO_2 through a laser drilled mircohole.

The expansion at the mircohole takes place adiabatically, i.e without heat transfer to the surrounding material inside the mircohole. There is just a temperature decrease in the

flow medium. This phenomenon is called the Joule-Thomson effect. This is largely based on the binding energies between atoms and molecules - the so-called van der Waals forces. For CO_2, the substance-specific Joule-Thomson coefficient is 1.1K / bar [4]. This means that during an expansion the medium cools down by 1.1 K per bar. When the CO_2 at the exit of the microholes expands freely to atmospheric pressure, it cools to 194.65 K and forms the described dry ice.

Nozzle shapes are generally divided into two types of geometry, a confusor and a diffuser. The diffusor gradually widens its cross section in the flow direction, the confusor becomes narrower (see Figure 5).

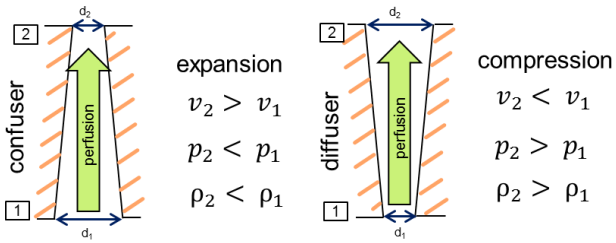

Figure 5. Comparison between confuser and diffusor .

The laws of mass conservation apply:

$$\dot{m} = \rho * \dot{V} = \rho * A * \vartheta = \rho * \frac{\pi}{4} d^2 * \vartheta \qquad (1)$$

$$\dot{V} = \frac{\pi}{4} d^2 * \bar{\vartheta} = constant \qquad (2)$$

From this, it follows that:

$$d_1 * \bar{\vartheta}_1 = d_2 * \bar{\vartheta}_2 \qquad (3)$$

Here, the term for the diffusor as a widening nozzle shape in flow direction is retained regardless of the flow rate. The same applies to the confusor as tapering nozzle geometry in flow direction (Figure 4).

The microholes were drilled with the laser in order to allow arbitrary shaping of the holes according to the needs described before. However, drilling of very deep microholes holes with the laser is not yet established and requires special attention due to basic physical limits which determine the resulting quality.

3. BASIC LASER DRILLING LIMITS

Laser-drilling of deep holes into tool steel is challenging: On the one hand, tool steel suffers from local phase transformation when the temperature exceeds 600 K. On the other hand, drilling of micro holes with high aspect ratio requires specific considerations regarding energy distribution in the capillary. Decreasing quality with increasing depth of the holes was observed and reported in numerous publications, e.g. in [5]. One of the major reasons for reduced quality during laser processing with ultra-short laser pulses is the so-called heat accumulation [6]. In addition, the limited pulse energy limits the maximum drilling depth: With increasing hole depth the total surface area of the wall of the microhole increases. This means that the average laser fluence (i.e. the laser pulse energy divided by the wall surface area) decreases. If the average fluence reaches the ablation threshold fluence, only very slow and localized drilling can occur. This limit is called "quality depth limit" in the following.

Heat accumulation and the quality depth limit were investigated for the required geometry of the microholes. For the experiments, the prototype kW-class ps-laser of the IFSW was used [7]. The passive disk-amplifier of this laser allows very high pulse energies which are necessary for laser drilling of deep holes. The diameter of the holes was adjusted with a helical drilling optics. This optics moves the beam on a circle with adjustable diameter. Furthermore, the optics allows adjusting the inclination angle of the beam relative to the surface which is necessary for longitudinal shaping of the holes. The properties of the laser, the helical drilling optics, and the focusing optics are summarized in Table 2.

Table 2. Properties of the IFSW kW-class-ps laser system and the helical drilling optics.

IFSW kW-ps laser	
Pulse duration	8 ps
Wavelength	1030 nm
Average power	≤ 650 W
Max. Pulse energy	≤ 2.2 mJ
Repetition rate	≤ 300 kHz
M^2	< 1.3
Polarization	Linear
Collimated beam diameter	5.2 mm
Helical drilling optics (GL-Trepan, GFH GmbH)	
Rotation speed	0-30'000 rpm
Hole diameters	0-1500 µm
Inclination angle	0°-4°
Focusing and ablation threshold	
Focal length	400 mm
Focus diameter	140 µm
Polarization	Circular
Focus position	On the surface
Max. Fluence	15 J/cm²
Ablation threshold (Steel, 8 ps, 1030 nm)	0.1 J/cm²

As it is described in Chapter 2, the inlet and outlet diameters of the microholes have to be 600 µm and 200 µm. Drilling microholes with a specific geometry needs precise moving of the laser beam. A laser drilling optic assists to fulfil this task. Here, we have used GL Trepan from GFH GmbH, Germany. The principle of a laser-drilling optic is described in [8]. As the collimated beam hits the focusing lens with a specific angle (relative to the optical axes of the lens), the focal point will be consequently at a certain distance of tens to hundreds of micrometer from the optical axis. If the collimated beam revolve in a circular route on the surface of a lens, the focal point will revolve on the surface of work piece. Therefore depends on the inclination angle of collimated beam and focal distance of the lens, the revolving diameter can be precisely adjusted.

3.1 Heat accumulation

Heat accumulation was identified as one of the major quality-reducing effects for deep-hole drilling [5].
The laser system that was described above was used to determine the limits where heat accumulation effects begin to reduce the quality. The optically measurable occurrence of phase transitions in the material was defined as an indicator for a reduced quality. These phase transformations include the formation of melt ($T \approx 1500$ K) as well as a solid phase transformation ($T \approx 600$ K). While the formation of melt is visible on the sample surface, the solid state phase transformations were analyzed by polishing and etching of the cross sections with Nital 5% for 40 seconds.
Figure 6 shows the effect of a decreasing repetition rate on heat affected zone and the drilling progress for a constant pulse energy of 2.2 mJ. At 300 kHz and an average power of 660 W the depth of the microhole was about 8 mm after $5 \cdot 10^5$ pulses (2 s of drilling time) (Figure 6a). However, a large heat-affected zone of about 1 mm can be seen. If the repetition rate is reduced to 100 kHz (which leads to an average power of 220 W), the hole depth after $1 \cdot 10^6$ pulses (10 s of drilling time) was reduced to about 5 mm. A heat affected zone is still visible as a bright area at the walls and in particular in the bottom of the hole (Figure 6b). Further reducing the repetition rate to 60 kHz yielded the same hole depth of about 5 mm after $1 \cdot 10^6$ pulses (17 s of drilling time) but without a visible heat affected zone and good hole quality.

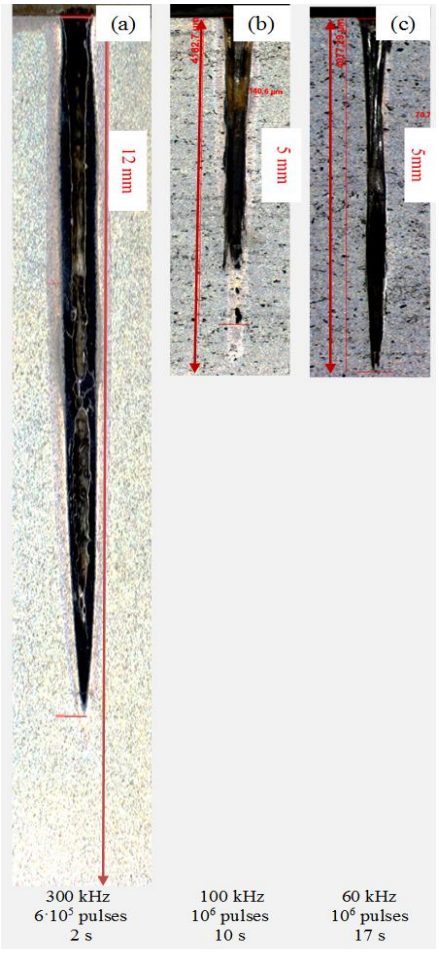

Figure 6. Cross-sections of laser-drilled microholes with a pulse energy of 2.2 mJ. All samples were etched with Nital 5% for 40 seconds.

These results lead to the conclusion that 60 kHz is the limiting frequency at the pulse energy of 2.2 mJ to maintain high quality of the drilled holes.

It is worth to mention that when drilling with a repetition rate of 300 kHz, melt ejection contributes to the drilling process. However, melt ejections lead to a reduced quality of the hole. Figure 7 shows ejected melt on the inlet of the microholes.

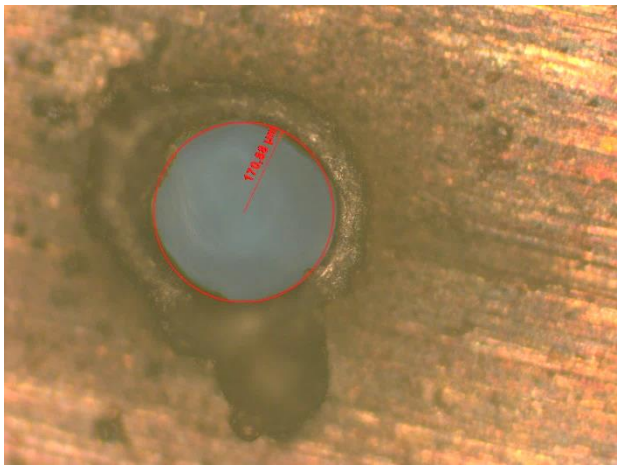

Figure 7. Melt ejection contributes to drill deeper using 300 kHz, however, a resolidified ring around the inlet is visible.

3.2 Depth limit

The hole depth as a function of the number of laser pulses for different repetition rates is shown in Figure 8. The pulse energy was 2.2 mJ.

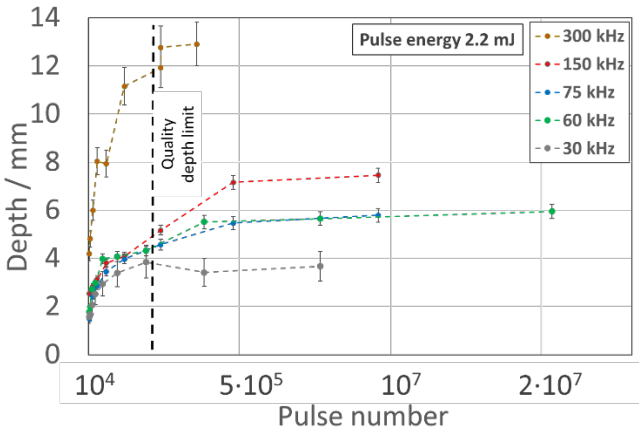

Figure 8. Hole depth as a function of the number of pulses for the pulse energy of 2.2 mJ for different repetition rates.

The drilling progress is very similar for repetition rates of 150 kHz and below. In the beginning of the drilling process, up to about $1 \cdot 10^5$ pulses, the drilling progress is very fast down to a depth of about 4 mm. As the depth increases, the process becomes slow and irregular. The faster drilling progress for $>2 \cdot 10^5$ pulses for the frequencies >30 kHz suggests, that heat accumulation gains influence after a very large number of pulses. It can be concluded that the above-mentioned "quality depth limit" is reached at about 4 mm for pulse energies of 2.2 mJ (marked by the dashed line in Figure 8).

4. LASER DRILLING OF MICROHOLES IN THE DEEP-DRAWING TOOL

4.1 Requirements

A sketch of the required geometries of the microholes are shown in Figure 9. The required hole depths and angles of the holes with respect to the surface of the deep drawing tool can be seen. The depth of the holes was either 5 mm or 6.7 mm, depending on the position of the hole in the tool. The angle of the hole relative to the tool surface was either perpendicular or 35°. In total, 254 microholes were drilled.

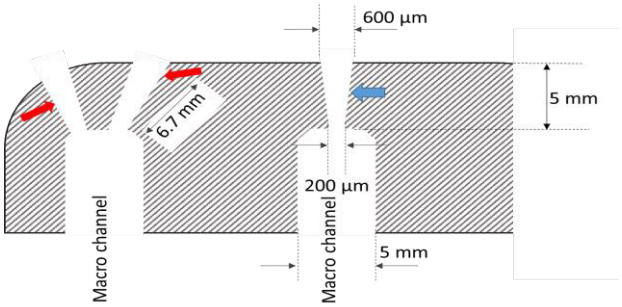

Figure 9. Geometry and position of the microholes: depth of 5 mm for perpendicular (assigned with blue arrow) and depth of 6.7 mm for angled microholes (assigned with red arrows). The microholes are connected to the macro channel which were manufactured by conventional mechanical tool.

As the required depth exceeded the above-discussed quality depth of 4 mm, we have to apply much more number of pulses to drill through. Inevitably, the extra amount of energy will be deposited into the capillary. To minimize the risk of damage, an additional break time should be apply to the drilling strategy to optimize the hole quality: After drilling for 0.5 s a break was introduced. The required duration of the break was determined experimentally. Figure 10 shows that decreasing the break between the drilling intervals from 2.0 s to 0.5 s results in the appearance of dross around the hole on the surface of the sample, marked with a red arrow.

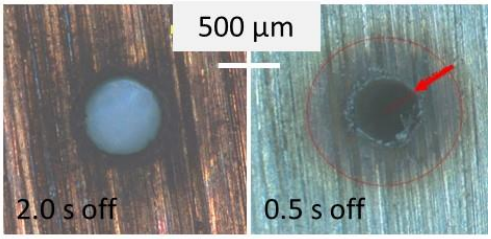

Figure 10, Decreasing the break between the drilling intervals of 0.5 s from 2.0 s to 0.5 s results in the appearance of dross on the surface of the sample, marked by the red arrow.

The influence of the longitudinal shape of the microholes feeding the liquid gases was discussed in Chapter 2. For the deep drawing tool the microholes shoud be diffusor-shaped with an output diameter of 600 µm and an input diameter of 200 µm. The longitudinal shaping of the hole was done with a helical drilling optics.

4.2 Laser-drilled microholes

Based on the results of the basic investigations described above, the microholes in the deep drawing tool were drilled with 60 kHz, the maximum available pulse energy of 2.2 mJ, and the above-mentioned drilling strategy of a 0.5 s drilling interval follow by a 2.0 s break (for the depth of 6.7 mm). In Figure 11, typical cross-sections of the laser-drilled, deep microholes suitable for the deep drawing application are shown.

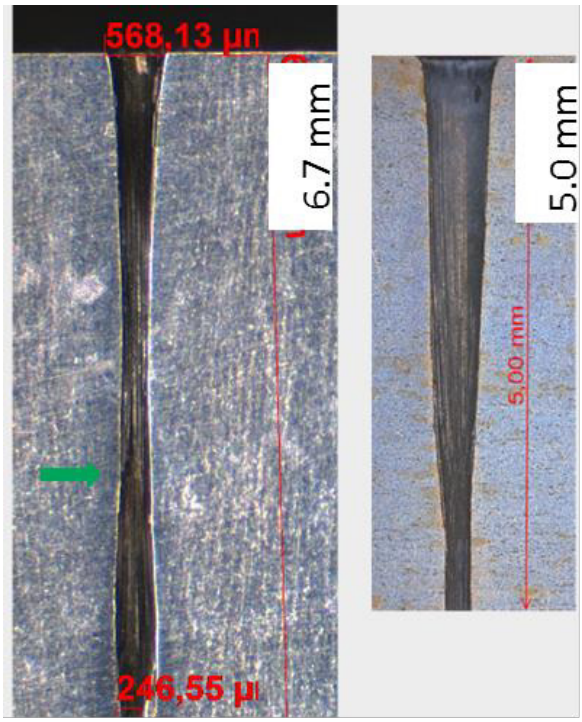

Figure 11. Typical cross-sections of the laser-drilled, 6.7 mm (left) and 5 mm (right) deep microholes for the deep drawing application. The green arrow indicates the "quality depth limit", the red arrow the widening of the hole due to the very long drilling time.

The net drilling time was 60 s and 320 s for the 5 mm and the 6.7 mm holes, respectively. Although the depth of 6.7 mm was reached, the respective drilling time was very long. That the quality depth limit was exceeded manifests in the longitudinal shape of the hole as seen in Figure 10. Down to a depth of about 4 mm (marked with a green arrow), the shape is conical and very regular. This depth corresponds to the "quality depth limit" as described above. For depths larger than 4 mm, the very long drilling time leads to an irregular widening of the hole cross-section. However, the holes were free of heat affected zones and free of burr on the surface. Overall, the quality was acceptable for the deep drawing experiments.

4.3 Manufacturing of the deep drawing tool

The completely drilled deep drawing tool is shown in Figure 12.

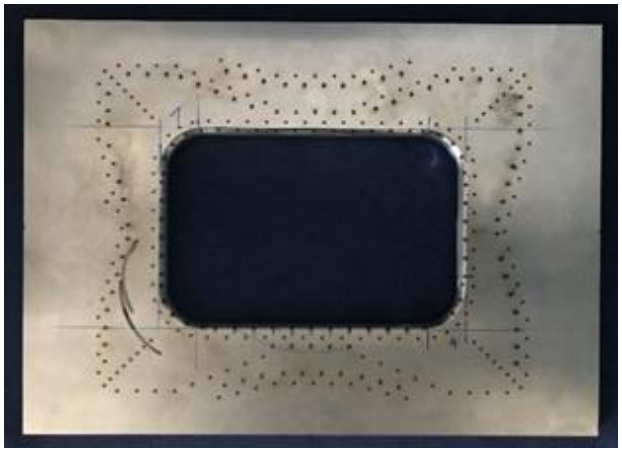

Figure 12. Processed deep drawing tool.

Due to constraints of the micro-processing station, positioning of the blank with respect to the absolute coordinates of the holes and the angle relative to the surface was done manually using auxiliary tools. This caused in particular inaccuracy of the focus position relative to the surface of the blank, which resulted in scattering of the hole diameters of about ±15%.

5. STRIP DRAWING INVESTIGATIONS

5.1 Experimental Setup

In order to evaluate the lubricating effect of gases during deep drawing, a strip drawing testing rig was modified to determine the coefficient of friction under different conditions in such way that the fluid could be induced into tool contact zone with work piece via laser-drilled micro holes inserted in strip drawing jaws, as it is shown in Figure 13.

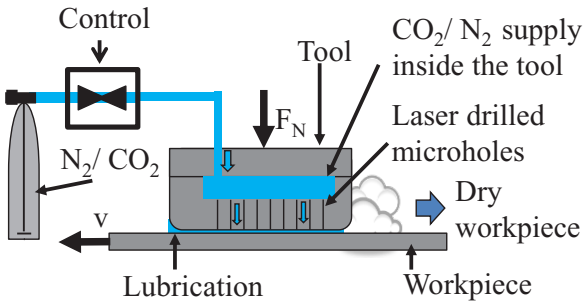

Figure 13. Experimental setup of strip drawing test using volatile media.

With the help of this test rig, various parameter combinations, such as nozzle type, borehole arrangement, borehole diameter, contact normal pressure, drawing speed and fluid pressure could be investigated for their influences. For all executed strip drawing investigations electrolytic galvanized sheet material DC05 was used. Because carbon dioxide in the conventional gas cylinder is present as a 2-phase area, where gaseous and liquid CO_2 are present at the same time. CO_2 is taken out of a standard gas bottle in liquid state, so that the pressure cannot be adjusted and remains constant depending on level of exit temperature. The pressure of nitrogen is set to the same value as for carbon dioxide at the supply valve (T=20°C, p≈ 60 bar) to maintain comparability.
The strip drawing test is an experimental model to investigate the influence of different parameters on the friction coefficient. However, the elastic and plastic deformations of the sheet metal material that occur in the actual deep-drawing process (e.g. thickness reduction) cannot be reproduced. Nevertheless, this experiment is very suitable for determining the qualitative influences of the individual parameters.

5.2 Results of strip drawing experiments

In order to gain a better understanding of the interdependencies of the tribological system using volatile media as lubricant substitutes, a large number of parameters were investigated [9, 10]. The following gives a compact overview of the results obtained from the strip drawing experiments.

The effects of number of conical holes (3, 7, 9, 21) and the diameters of (200 µm, 600 µm) and nozzle types (diffuser, confuser) were investigated. The main effects of these parameters on the coefficient of friction are depicted in Figure 14 and Figure 15.

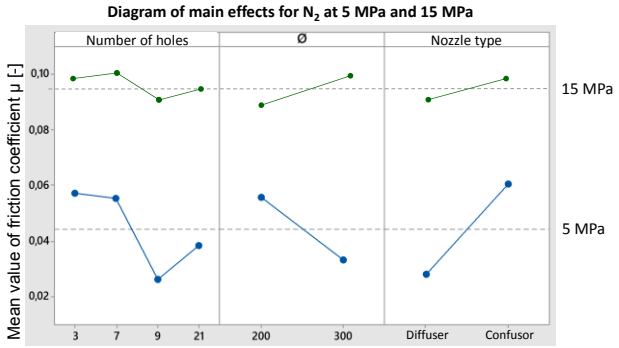

Figure 14. Main effects on coefficient of friction µ determined with strip drawing investigations at 5 MPa (lower, blue values) and 15 MPa (higher, green values) surface pressure, drawing speed 100 mm/s, lubrication medium N_2, All values represent averaged values for the respective configurations.

Using nitrogen (N_2) or carbon dioxide (CO_2) as lubrication a significant reduction of the friction coefficient is achieved at low contact pressure (5 MPa) with an increasing number of bores. In the tests with 21 holes using N_2, friction increases slightly again, which can be justified by the fact that the pressure in the supply channels decreases sharply due to the increased outflow of the gas with a large number of holes and therefore a lubricating effect is only achieved in a weakened manner. CO_2 is not that sensitive on the diameters of the supply channels, because the specific volume increase at 20°C, due to the phase change from liquid to gaseous, is nearly four fold. That's why decreasing pressures in the supply channels will occur at markedly higher output rates of CO_2 compared to N_2.

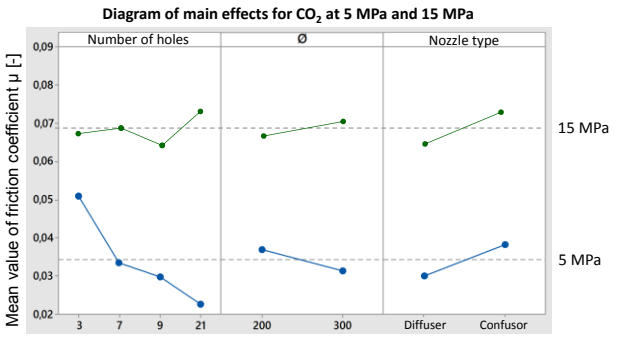

Figure 15. Main effects on coefficient of friction µ determined with strip drawing investigations at 5 MPa (lower, blue values) and 15 MPa (higher, green values) surface pressure, drawing speed 100 mm/s, lubrication medium CO_2, All values represent averaged values for the respective configuration.

For both fluids, diffusors obtain lower friction coefficients at 5 MPa as well as at 15 MPa. This result was used, among all the experiments, for the design of the forming tool of the rectangular cup and so there all laser-drilled microholes were drilled as diffusers [11]. Dashed lines in both diagrams represent the averaged value of all friction coefficients obtained by strip drawing experiments at a contact pressure of 5 MPa and 15 MPa. As can be seen in the diagrams, CO_2 achieves lower averaged friction values than N_2 at both high and low surface pressures. A possible explanation of this effect could be the formation of dry ice. To get a better understanding of these effects, further investigations on the effects of dry ice formation when using CO_2 as a lubricant substitute [9] and the pressure conditions in the tool contact zone [11] were carried out in the course of this research work.

6. DRY DEEP DRAWING OF A RECTANGULAR CUP

Tool design

In order to reduce the drilling depth for the laser process without reducing the tool strength a segmented tool design was chosen (see Figure 2). The base plate contains the holes for the media supply and a sealing to avoid an uncontrolled flow out between the plates while the upper plate contains different supply channels and laser-drilled microholes. The position of the supply channels determines the location of microholes. In order to avoid a free flow out of the media through the microholes at the end of the forming process the position of the supply channels was optimized using a sheet metal forming simulation of the blank draw-in. As a result, one ring channel was integrated next to the die radius and four additional channels are arranged with regard to the blank draw-in. Each supply channel can be controlled separately by a valve to stop free flow out of liquid during deep drawing.
One row of microholes was drilled perpendicular into the supply channel having a depth of 5 mm and one row was incorporated by an angle of 35° and a length of around 7 mm. Additional microholes were placed in the die radius area. In total, 154 microholes were distributed over the tool surface of the die. For the blankholder, the same design was chosen though without radius. Here about 100 microholes were drilled into the tool.

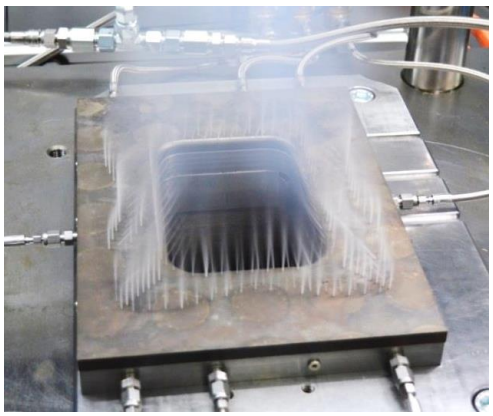

Figure 17. Free flow out of the CO_2 through laser-drilled microholes in the die of the deep drawing tool.

Due to some problems in the tool manufacturing, it was necessary to re-mill the die radius after die laser drilling. For this purpose, the tool was connected to a compressed air system applying a pressure level of 2 bar during the

milling process. By doing so, surprisingly none microhole was blocked due to the machining process. Also after the final hardening process of the tool, no blockage of the microholes could be observed. The final assembly of the die tool is shown in Figure 17 while a free flow out of the CO_2 through the laser-drilled microholes is activated.

6.1 Experimental setup

In order to understand the limits of this new tribological system, several deep drawing tests have carried out and compared with conventional deep drawing process using mineral oil- or wax-based lubricants. An established method is the determination of the process window. Usually, the blank holder force and the drawing ratio is varied in the deep drawing process in order to find maximum drawing depth without wrinkles or cracks. By doing so, the valid process window can be determined where no cracks and no wrinkles in the flange area appear. For non-rotational parts the drawing depth is used instead of the drawing ratio.

All drawing experiments were carried out using electrolytic galvanized sheet material DC05. The sheets were cleaned manually and then degreased in an acetone bath in order to remove remaining oil on the sheet. Liquid CO_2 having an initial pressure level $p_{initial}$ of 60 bar and gaseous N_2 at the same pressure level were used as temporarily acting lubricant for dry metal forming. The supply of the media was controlled by the ram movement. The supply was switched on in the moment of the first contact between the tool and the sheet and shut down at the bottom dead center of the press. Additionally, drawings with the lubricant Wisura ZO3368 (1.5 g/m²) were investigated using the same tool. All tests were carried out on an AIDA servo press at a ram speed of 6 strokes per minute which corresponds approximately to 100 mm/s at the beginning of the forming process.

6.2 Experimental results und discussion

Presented approach for dry metal forming was tested successfully and so, a rectangular cup was deep drawn using N_2 and CO_2 as temporarily acting lubrication for the very first time. In accordance with former tests results investigating the coefficient of friction [10] and the deep drawing of a U-shaped profile geometry [9], the new lubrication system performed better than the conventional one using a mineral oil-based lubricant (see Figure 18).

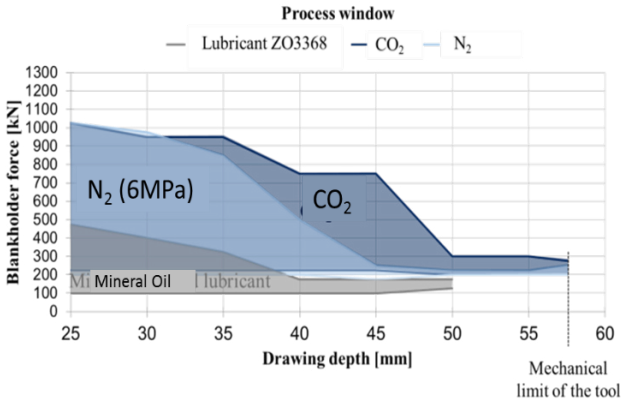

Figure 18. Process windows for deep drawing of a rectangular cup using different lubrication systems.

The maximum drawing depth could be increased to 57.5 mm by using CO_2 and N_2. This depth corresponds to the mechanical limit of the tool. By using lubricant ZO3368 only 50 mm as a maximum drawing depth was achieved. Also the fracture limit was raised up to 50% depending on the drawing depth by using CO_2 as well as N_2. Thereby, CO_2 performs better for deeper cups than N_2. It is assumed that this is caused by different pressure levels acting in the gap between the sheet and the tool resulting by the different media [11]. In general this pressure in the gap p_{gap} is influenced by microholes (position, numbers, nozzle type), the initial pressure level of the injected media $p_{initial}$ and the sealing effect between tool surface and the sheet. Also the sealing effect is influenced by many factors such as the blankholder force $F_{Blankholder}$, the tool and sheet surface roughness and the thinning and thickening of part flange during deep drawing. Finally, there are interactions between the sealing effect, the pressure level p_{gap} and the height of the mean gap h_{gap} between the sheet asperities and the forming tool. A schematic illustration of the conditions in the gap and the applied designations are shown in Figure 19.

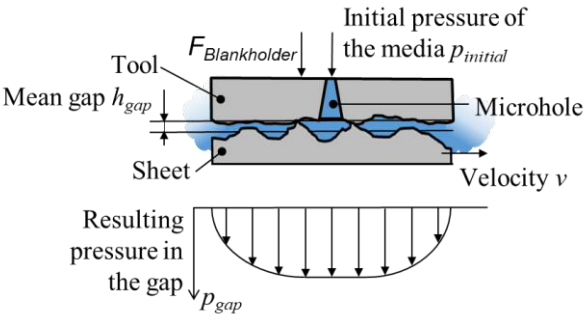

Figure 19. Schematic illustration of the resulting pressure between sheet and tool.

By deep drawing with volatile media acting as lubrication not only the fracture limit, but also the wrinkle limit was increased noticeably (see Figure 18). Also this effect can be explained by the assumption that the mean gap h_{gap} and the pressure p_{gap} mainly do influence the sheet metal forming behaviour. For lower blank holder forces a higher gap h_{gap} occur without or with minimum contact areas between the tool and the sheet asperities. While forming, wrinkles of 1st order develop due to increasing tension stress in the blank without prevention by the blank holder. Thereby, the pressure in the gap, which is a scalar quantity acting in all directions, cannot avoid the local development of wrinkles. The outflowing gas through the wrinkles support such development additionally. Other tests indicate that the wrinkle limit is raised further by using a pressure $p_{initial}$ of N_2 higher than 60 bar. However, also the fracture limit can be increased extremely. This confirms the assumption that the resulting pressure level p_{gap} of the volatile media between the sheet and tool mainly influences the friction behaviour and therefore the forming limits in the deep drawing process of this new approach.

In addition to those investigations on process limits in deep drawing, the cooling effect on the sheet surface caused by the Joule-Thomson effect during the relaxation

of CO_2 and N_2 was investigated. The temperature was measured visually after the deep drawing process using a thermal camera.

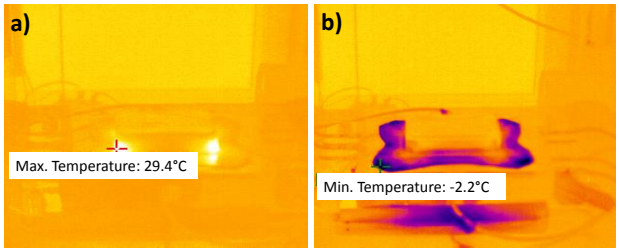

Figure 20. Measured temperature on the sheet surface after deep drawing using (a) nitrogen and (b) liquid carbon dioxide as lubricant.

In Figure 20, the visualized temperature is shown using nitrogen (a) and liquid carbon dioxide (b) as lubricant for the same process having a drawing depth of 35 mm and a blank holder force of 275 kN. The maximum measured temperature (29.4°C) after deep drawing using nitrogen is almost similar to the sheet temperature when using mineral oil-based lubricants (30.1°C). The heating in the corner of the cup is caused by dissipating forming energy and friction heat. By contrast, using liquid CO_2 as temporally acting lubricant reduces the sheet temperature in the flange area down to -2.2°C (see Figure 20(b)). Compared to the first deep drawing experiments using a U-profile geometry [8], a cooling effect of only a few degrees Celsius were measured. The cooling effect merges much more significantly when deep drawing the rectangular cup. Additional to that the control of valves also plays an important role. Finding the right timing to switch on and off the flow of media appear more complex for the drawing process of a rectangular cup having curved arrangements of microhole positions onto the tool surface and more complex draw-in compared to previous drawn part as described. Another reason might be given by effect of changing flange thickness during drawing counteracting to local blank holder force. Small gaps between the tool and the sheet induced by small wrinkles of 1st order can occur supporting the flow out of the CO_2 and therefore the cooling of the sheet due to high velocity of media. According to these results, the flow control and also the position of microholes have to be optimized in further research work in order to reduce observed extreme cooling of the sheet. A different approach is given to use the cooling effect actively to reduce the heating in drawing process, while heating of parts due to friction heat and dissipating forming energy is undesirable.
However, overall presented results show that a dry forming by means of temporally acting volatile media is possible, which not only allows an equivalent substitution of mineral oil-based lubricants, but also an enhancement of the process limits in sheet metal forming. Especially using nitrogen with a pressured level adjusted to the respective process conditions are extremely promising.

Conclusions

The progress in the use of volatile media as lubricant substitutes in the deep drawing process in this paper was demonstrated based on achieved results. Thus, numerous technological challenges in the manufacturing of precise micro-drilling by laser drilling were mastered, but also deepened knowledge could be gained experimentally and simulatively by examining emerging friction conditions in the tool contact zone. Furthermore, after deep drawing of approximately 300 cups under dry as well as lubricated conditions no microholes were blocked by zinc abrasion or other effects. So it can be assumed that blockage of the microholes is not a limitation factor for this new approach. In a next step, these results have to be confirmed by prospective deep drawing endurance tests. Further performed measures also will be implemented into the test stand in the coming funding period. The tool radii of a new testing rig, which are subjected to high friction and wear loads, will be provided with feedholes for volatile media flow too. Complex friction conditions in corner areas and interaction with deep-drawing process will be investigated in this new special testing rig. A further goal of future research is to expand the range of applications for zinc-coated steel sheets to include selected aluminium sheet materials, which poses enormous challenges with regard to a more complex tribological system and its susceptibility to failure. Furthermore, the theoretical knowledge of the friction behaviour of volatile media in the tribological system is to be further deepened in order to understand and specifically influence the occurring effects and thus to ensure robust and stable deep drawing processes.

Acknowledgement

The scientific investigations of this paper are funded by the German Research Foundation (DFG) within the priority program SPP 1676 Dry Metal Forming - Sustainable Production by Dry Processing in Metal Forming.

References

1. F. Vollertsen, F. Schmidt, “Dry Metal Forming: Definition, Chances and Challenges,, IJPEM-GT, **1**, 59-62 (2014).
2. Kapler, P.: Partikelbildung und -morphologie bei der Hochdruckmikronisierung gashaltiger Lösungen, Dissertation, Ruhr-Universität Bochum, 2002.
3. Fachlabor UTRM SoSe 2010, Hochdruckextraktion mit CO2.
4. Atkins, P. W. and de Paula J., “Physical Chemistry“ Oxford University Press, 10th Revised Edition, Oxford, 2014.
5. S. Döring, S. Richter, A. Tünnermann, S. Nolte, “Evolution of hole depth and shape in ultrashort pulse deep drilling in silicon", Appl. Phys. A **105**, 69–74, (2011).
6. R. Weber, T. Graf, P. Berger, V. Onuseit, C. Freitag, M. Wiedenmann, A. Feuer, “Heat accumulation during pulsed laser materials processing”, Optics Express **22**

(9), 11312–11324 (2014), and Erratum thereto in Optics Express 22 (23), 28232, (2014).

7. J. P. Negel, A. Voss, M. Abdou ahmed, D. Bauer, D. Sutter, A. Killi, T.Graf. "1.1 kW average output power from a thin-disk multipass amplifier for ultrashort laser pulses", Optics Letters **38**, 5442-5445, (2013).
8. S. Nolte, F. Schrempel, F. Dausinger, *Ultrashort Pulse Laser Technology,* 201-205, (2016).
9. C. Woerz, E. Zahedi, G. Umlauf, M. Liewald, R. Weber, T. Graf, G. E. M. Tovar, "Tiefziehen eines U-Profils mit flüchtigen Medien als Schmierstoffer- satz", Dry Met. Forming OAJ FMT, **3**, 50-61, (2017).
10. C. Woerz, M. Liewald, M. Singer, "Investigation of Tribological Conditions in the Strip Drawing Test Using Liquid CO_2 and N_2 as a Volatile Lubricant", *Proceed. of 7th ICTMP*, 140-148, (2016).
11. C. Woerz, G. Reichardt, M. Liewald, E. Zahedi, R. Weber, T. Graf, "Dry deep drawing of a rectangular cup assisted by volatile media injected from laser-drilled microholes" Dry Met. Forming OAJ FMT, **4,** (2018).